WAPD-T--3218
CONF-981055--

Optical Properties of Thin Semiconductor Device Structures with Reflective Back-Surface Layers

Marvin B. Clevenger, Westinghouse Electric Company
Christopher S. Murray, Westinghouse Electric Company
Steven A. Ringel, Ohio State University
Robert N. Sachs, Ohio State University
Linhong Qin, Ohio State University
Greg W. Charache, Lockheed Martin Inc.
David M. Depoy, Lockheed Martin Inc.

DE-AC11-93PN38195

NOTICE

This report was prepared as an account of work sponsored by the United States Government. Neither the United States, nor the United States Department of Energy, nor any of their employees, nor any of their contractors, subcontractors, or their employees, makes any warranty, express or implied, or assumes any legal liability or responsibility for the accuracy, completeness or usefulness of any information, apparatus, product or process disclosed, or represents that its use would not infringe privately owned rights.

MASTER

DISTRIBUTION OF THIS DOCUMENT IS UNLIMITED

Optical Properties of Thin Semiconductor Device Structures with Reflective Back-Surface Layers

M. B. Clevenger and C. S. Murray
Westinghouse Electric Company, West Mifflin, PA 15122

S. A. Ringel, R. N. Sachs and L. Qin
Department of Electrical Engineering
Ohio State University, Columbus, OH 43210-1272

G. W. Charache and D. M. Depoy
Lockheed Martin, Inc., Schenectady, NY 12301-1072

Abstract. Ultrathin semiconductor device structures incorporating reflective internal or back surface layers have been investigated recently as a means of improving photon recuperation, eliminating losses associated with free carrier absorption in conductive substrates and increasing the above bandgap optical thickness of thermophotovoltaic device structures. However, optical losses in the form of resonance absorptions in these ultrathin devices have been observed. This behavior in cells incorporating epitaxially grown FeAl layers and in devices that lack a substrate but have a back-surface reflector (BSR) at the rear of the active layers has been studied experimentally and modeled effectively. For thermophotovoltaic devices, these resonances represent a significant loss mechanism since the wavelengths at which they occur are defined by the active TPV cell thickness of ~2-5 microns and are in a spectral range of significant energy content for thermal radiators. This study demonstrates that ultrathin semiconductor structures that are clad by such highly reflective layers or by films with largely different indices of refraction display resonance absorptions that can only be overcome through the implementation of some external spectral control strategy. Effective broadband, below-bandgap spectral control using a back-surface reflector is only achievable using a large separation between the TPV active layers and the back-surface reflector.

Introduction

Previously, photovoltaic and thermophotovoltaic (TPV) cells have been shown to benefit significantly from the introduction of highly reflective layers at the back surfaces of devices [1-2]. In these applications, the back surface reflector (BSR) serves a number of important functions. The BSR increases the above-bandgap optical thickness of device structures by providing multiple internal reflections of incident light, aids in the recuperation of below-bandgap light (important in TPV) and, when incorporated into the device above the substrate, eliminates losses associated with free carrier absorption in conducting substrates and heavily doped layers used for lateral current conduction. In this work, two strategies for the use of BSR's were investigated in order to improve the performance of TPV devices.

First, the fabrication of UltraThin TPV (UTTPV) cells was investigated wherein the p-InP substrates of 0.74 eV and 0.55 eV single junction TPV devices were replaced with unalloyed gold back contacts. This work was completed using a peeled epitaxial lift-off process or a chemical etching process for InP substrate removal followed by thermal deposition of the gold back surface reflector/contact. This strategy left an n-on-p InGaAs TPV cell backed by a gold BSR/contact layer.

DISCLAIMER

This report was prepared as an account of work sponsored by an agency of the United States Government. Neither the United States Government nor any agency thereof, nor any of their employees, makes any warranty, express or implied, or assumes any legal liability or responsibility for the accuracy, completeness, or usefulness of any information, apparatus, product, or process disclosed, or represents that its use would not infringe privately owned rights. Reference herein to any specific commercial product, process, or service by trade name, trademark, manufacturer, or otherwise does not necessarily constitute or imply its endorsement, recommendation, or favoring by the United States Government or any agency thereof. The views and opinions of authors expressed herein do not necessarily state or reflect those of the United States Government or any agency thereof.

DISCLAIMER

Portions of this document may be illegible in electronic image products. Images are produced from the best available original document.

The second strategy employed was the replacement of the lateral conduction layer (LCL) in a Monolithic Interconnected Module (MIM) with a buried, epitaxial layer of FeAl. This technique of incorporating a highly reflective layer into the TPV cell architecture, above the substrate, offered the above-stated advantages afforded by the use of BSR's while also minimizing the series resistance normally associated with the semiconducting LCL. This work was completed through the epitaxial thermal evaporation of iron and aluminum to yield a $Fe_{0.5}Al_{0.5}$ alloy that is lattice matched to InP, followed by the growth of a *p-on-n* InGaAs TPV cell structure.

These types of TPV structures exhibit similar optical responses. Notably, destructive interference patterns are established as a result of the effective TPV cell thickness being on the order of incident wavelengths. Similar behaviors have been observed previously in photovoltaic structures where light trapping for increased optical pathlength was an objective [2]. However, in thermophotovoltaic structures, such resonance absorption bands decrease significantly the devices' spectral utilization factors [3] and overall efficiencies. Described herein are efforts to model and measure this optical behavior in UTTPV cells and those incorporating buried metal layers.

Optical Modeling Method

The optical response of ultrathin TPV cells was modeled using the commercially-available code TFCalc.™ In order to accurately predict the optical response of a multilayer structure, TFCalc™ requires that the wavelength dispersion of the refractive index (n) and the extinction coefficient (k) be entered in tabular form or be specified by identifying accurately the coefficients for a dispersion equation (e.g. the Drude formula). For the TPV cell structures modeled in this work, n and k data tables were generated using two methods. For undoped InGaAs, n-InGaAs, some p-InGaAs and undoped InP layers, n and k data was calculated from front surface reflectance measurements [3]. For other p-InGaAs and doped InP layers, n and k data acquired via spectroscopic ellipsometry was used [4]. In either analysis method, the production of accurate, comprehensive data tables over a range of wavelengths can be difficult, and iterative comparison to experimentally obtained data is essential. The structure employed for the ultrathin TPV cell study is shown in Figure 1.

500Å $3x10^{18}$ n-InP
500Å $3x10^{18}$ n-InGaAs
2.1µm $2x10^{17}$ p-InGaAs
500Å $5x10^{18}$ p-InP
150Å $5x10^{18}$ p-InGaAs
30Å Palladium
1600Å Gold

Figure 1. Ultra-thin TPV cell structure used in modeling studies and reflectance measurements

The behavior of TPV cells incorporating epitaxially grown metal layers was also modeled. Here, the device structure shown in Figure 2 was used to model a TPV device with a Fe_xAl_{1-x} lateral conduction layer. The wavelength dispersions of n and k for the

1000Å $1x10^{19}$ p-InGaAs Emitter
3µm 0.74eV n-InGaAs Base
500Å $3x10^{18}$ n-InGaAs Back Surface Field
Buried Metal Layer
1200Å Undoped InGaAs
350µm InP Substrate

Figure 2. Device structure modeled using TFCalc.

semiconductor layers were acquired as described above for the UTTPV cells. The dispersions of the refractive index and extinction coefficient for Fe_xAl_{1-x} were obtained from calculations of the self-consistent band structure of FeAl [5] and Kramers-Kronig analysis of near-normal reflectance from $FeAl_{1-x}Cu_x$ [6]. The $FeAl_{1-x}Cu_x$ alloy possesses a dielectric constant and joint density-of-states that are in good agreement with the values obtained from band structure calculations for FeAl, and it has been shown that the substitution of copper for aluminum in FeAl does not change the band structure significantly [6]. As a result, both methods produced very similar results for the wavelength dispersion of n and k.

Results and Discussion

Modeled and measured reflectances for the ultrathin TPV cell structure are provided in Figure 3. Here, a pattern of destructive interference results in resonance losses across the infrared. This is a direct result of making the effective TPV cell thickness on the order of the wavelengths of incident light. Thus, it is important to note that photonic devices should have thicknesses substantially different from the wavelength of light in the region in which they are operating. This can be seen from the analysis below.

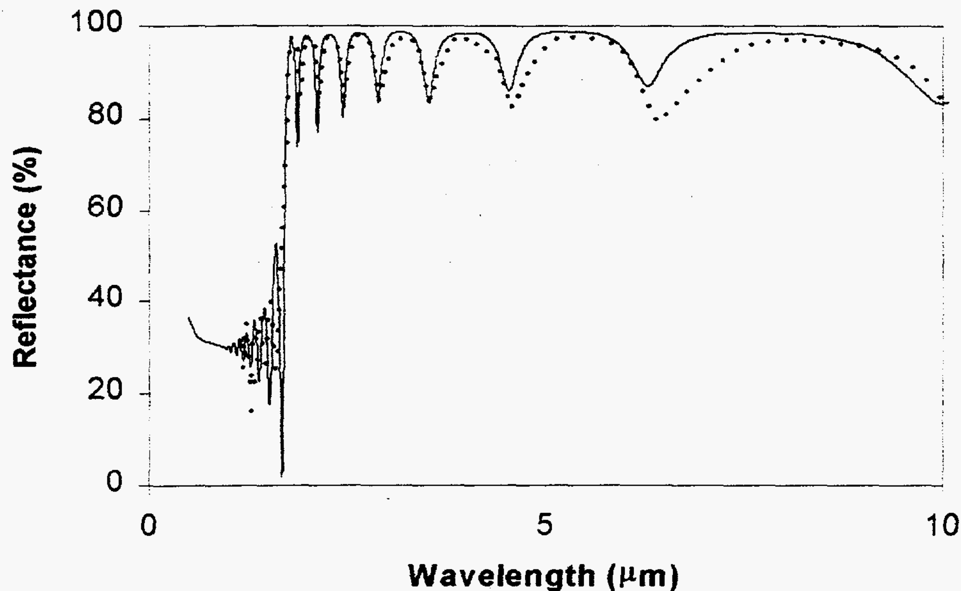

Figure 3. (—)Modeled and (•••)measured reflectance of an ultrathin TPV cell.

The resonance absorption bands displayed by the UTTPV sample exhibit a destructive interference pattern that can be described by the principle of superposition of waves [7-8]. Accordingly, for waves in phase that are incident on a cell, a reflected phase difference, δ, arises from a difference in the pathlength traveled by each wave:

$$\delta = \frac{2\pi(x_1 - x_2)}{\lambda} \qquad \text{Eq. (1)}$$

where x_1 and x_2 are the distances from the source of the two waves to the point of observation and λ is the wavelength in the medium (cell). The pathlength differences for individual waves propagating through a structure arise from partial reflectance of the waves at each interface in the structure. The reflectance at each interface can be evaluated using Equation (2):

$$R = \frac{(n_2 - n_1)^2 + k^2}{(n_2 + n_1)^2 + k^2} \qquad \text{Eq. (2)}$$

where n_1 and n_2 are the refractive indices of the incident medium and the layer being encountered at the interface, respectively, and k is the extinction coefficient of the layer being encountered. The total distance traveled by a wave through a structure will determine its phase difference with other waves within the structure. For example, depicted in Figure 4 are three of the possible paths through a UTTPV cell structure for incident light (I_0) with a wavelength of 1.1 μm. Because the reflected wave R_2 has traveled 4.4 μm farther than R_1 (2.2 μm into the device and 2.2 μm out), Equation (1) states that the two waves will be in phase. Arriving at the front surface in phase with R_1 means that R_2 will constructively interfere with R_1, and, assuming no absorptive losses, the intensity of the interference wave (R_1 + R_2) will match that of I_0. However, in the case of wave R_3, it has traveled a total of 4.536 μm farther than R_1. This will result in R_3 being ~45° out of phase with R_1. The resulting partial destructive interference will produce a decrease in net reflected intensity from the device at 1.1 μm.

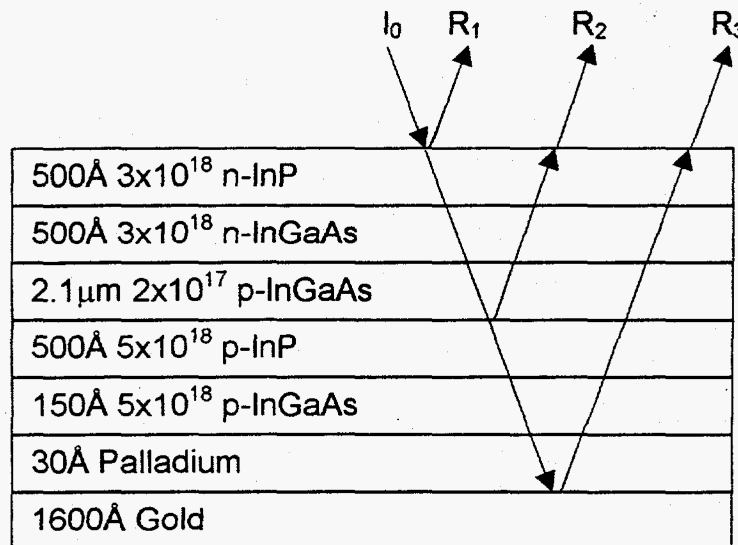

Figure 4. Schematic depicting different optical paths for an incident wave that will produce varying degrees of constructive and destructive interference.

In high index materials such as InP and InGaAs, it is useful to relate Equation (1) to the media through which the waves are propagating. Thus, given that the refractive index of each layer of the structure is $n=\lambda_0/\lambda$, where λ_0 is the wavelength of incident light in air, the phase difference between interfering waves at each interface is evaluated using Equation (3):

$$\delta = \frac{2\pi n(x_1 - x_2)}{\lambda_0} \quad \text{Eq. (3)}$$

For the thermophotovoltaic device structures under consideration here, two simplifications can be made in calculating phase differences and resultant reflected intensities. First, InP and InGaAs layers possess approximately equal indices of refraction in the infrared. Second, the incorporation of a reflective back surface or internal layer dictates that the principle reflection from within the device takes place at the interface to that layer. The ramification of these two facts is that calculations of the phase difference of waves exiting the TPV structure can be completed accurately by assuming that the multilayer TPV structure possesses a single dispersion of the refractive index (i.e. that it behaves as one thick layer) and that the quantity (x_1-x_2) is simply twice the cell thickness, t. Equation (3) is then simplified to:

$$\delta = \frac{2\pi n(2t)}{\lambda_o} \quad \text{Eq. (4)}$$

which can be applied effectively to the entire device without serious and tedious consideration being given to reflections at every interface. From Equation (4), it can be seen that complete destructive interference will always occur when $\delta=m\pi$, or

$$t = \frac{(2m+1)\lambda_0}{4n} \quad \text{Eq. (5)}$$

where m is an integer (m=1, 2, 3,...).

As stated previously, in thermophotovoltaic cells, the principle reflection is from the back-surface reflector or from a highly reflective layer that is incorporated into the device. When this highly reflective layer is behind the active layers of the device, the effective cell thickness is on the order of the wavelengths emitted by thermal radiators and the destructive interference patterns are established in the infrared. However, if a BSR is placed behind a thick substrate of a TPV cell, the major effective optical pathlength difference between any internal or surface reflections and that from the BSR will be on the order of 350 μm. This shifts significantly the destructive interference patterns out of the infrared region of the spectrum.

By a similar approach to that described above, the reflectance of a TPV cell incorporating a reflective internal layer can be modeled. When the optical behavior of a FeAl layer grown epitaxially above the cell substrate is modeled using the results of band structure calculations and Kramers-Kronig analyses, the results converge to yield a reflectance typical of that shown in Figure 5 [6]. As in the case of the ultra-thin TPV cells, a destructive interference pattern is produced by the superposition of waves reflected from each of the layers within the device, but principally from the reflective FeAl layer.

However, in the case of buried metal layers, there are greater losses associated with the destructive interference. These losses can be attributed primarily to the use of Group III-transition metal alloys as buried metal layers. Alloys of this kind are needed to

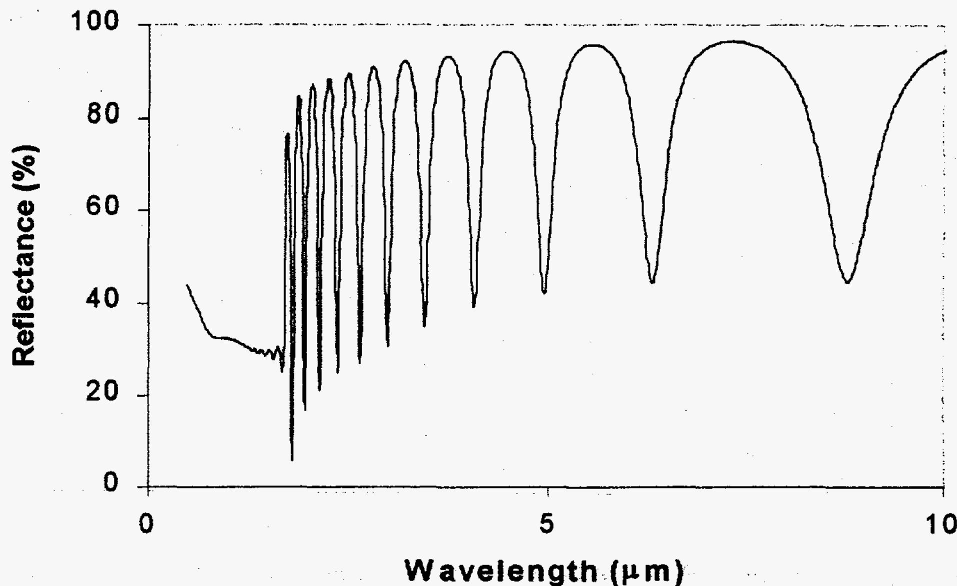

Figure 5. Modeled reflectance of a TPV cell incorporating a buried FeAl layer.

achieve an effective lattice match to InP substrates. However, the transition metal component, in this case iron, absorbs significantly in the infrared, particularly at wavelengths below 4 μm. Thus, the reflectance of buried metal layer structures is observed to decrease with wavelength.

Applying the analysis of destructive interference patterns detailed above, it is possible to predict accurately the location of resonance absorption bands for ultrathin structures and determine the reflection order, m, that is resulting in the loss. Assuming that the semiconductor layers within both the UTTPV and buried metal layer structures all possess dispersions of the refractive index that can be described by the Drude formula (i.e. they act as a single n-InGaAs layer), the locations of resonance absorption bands resulting from destructive interference were calculated using Equation (5). The results of these calculations are provided with the TFCalc™-predicted and experimentally determined values in Table 1.

From the results presented in Table 1, it is clear that destructive interference patterns in thin TPV structures may be predicted accurately. Optical models require knowledge of individual layer thicknesses, compositions and dopant densities and measurements require the growth and characterization of a sample in order to determine the location of resonance absorption bands that result from destructive interference. However, use of the equations that result from the principle of superposition allows the same determination to be made accurately from knowledge only of the total thickness and average refractive index of the structure. This approach should benefit significantly future efforts to either avoid or utilize light trapping structures in thermophotovoltaic and photovoltaic related applications.

Finally, the resonance losses associated with the destructive interference patterns established in UTTPV and MIM/buried metal layer structures can effectively be attenuated through the use of a front-surface filter. It is possible to utilize either a discrete interference or tandem filter to reflect above bandgap light back to the radiator for recuperation. If device spectral utilization and efficiency are to be maintained with an ultrathin TPV structure, front-surface spectral control is essential.

Table 1. Calculated, Modeled and Measured Wavelengths at Which Destructive Interference Occurred in Thin TPV Devices with Reflective Layers.

Reflection Order, m	Ultrathin TPV Cells			Buried Metal Layer Cells	
	Calculated (μm)	TFCalc (μm)	Measured (μm)	Calculated (μm)	TFCalc (μm)
1	9.95	9.98	10.00	12.95	-
2	6.25	6.28	6.39	8.45	8.79
3	4.55	4.55	4.58	6.20	6.33
4	3.55	3.57	3.57	4.90	4.94
5	2.90	2.92	2.94	4.05	4.05
6	2.50	2.48	2.50	3.40	3.43
7	2.15	2.15	2.17	3.00	2.98
8	1.85	1.90	1.86	2.65	2.63
9	-*	-	-	2.35	2.36
10	-	-	-	2.15	2.13
11	-	-	-	1.95	1.95
12	-	-	-	1.80	1.79

*Values below the bandedge of 0.74 eV cells.

Summary

The incorporation of reflective internal or back-surface layers into thermophotovoltaic devices offers a variety of advantages, including: an improvement of photon recuperation, an elimination of losses associated with free carrier absorption in conductive substrates and an increase in the above bandgap optical thickness of device structures. However, placing the highly reflective layers directly behind the active layers of a cell renders the effective device thickness comparable to the wavelengths emitted by thermal radiators. Consequently, a pattern of destructive interference is established that is governed by the principle of superposition. The multiple, absorptive layers that comprise a TPV device augment this problem. The resonance losses that result occur principally in the spectral range of significant energy content for thermal radiators and a device structure with a low spectral utilization results. In order to combat this problem effectively, a large separation between the cell active layers and the back-surface reflector must be maintained, or a broadband, front-surface spectral control strategy must be used.

[1] P. A. Ilies and C. L. Chu, *Proceedings of the 25th IEEE Photovoltaics Specialists Conference*, 1996, pp.109-112.

[2] M. G. Mauk, P.A. Burch, S. W. Johnson, T. A. Goodwin and A. M. Barnett, *Proceedings of the 25th IEEE Photovoltaics Specialists Conference*, 1996, pp. 147-150.

[3] M. B. Clevenger, C. S. Murray and D. R. Riley, *Proceedings of the 1997 Fall Meeting of the Materials Research Society*, 1997, in press.

[4] S. Adachi, *Physical Properties of III-V Semiconductor Compounds: InP, InAs, GaAs, GaP, InGaAs, and InGaP*, John Wiley and Sons, New York, 1992.

[5] C. Koenig and M. A. Khan, *Phys. Rev. B* **27**, 6129 (1983).

[6] A. S. Saleh and M. Y. Alaqra, *Solid State Comm.* **66**, 521 (1988).

[7] J. D. Ingle, Jr. and S. R. Crouch, *Spectrochemical Analysis*, Prentice Hall, New Jersey, 1988.

[8] J. I. Pankove, *Optical Processes in Semiconductors*, Dover Publications, New York, 1971.